

# The HECT E3 ligase Smurf2 is required for Mad2-dependent spindle assembly checkpoint

Evan C. Osmundson,<sup>1,3</sup> Dipankar Ray,<sup>1</sup> Finola E. Moore,<sup>1</sup> Qingshen Gao,<sup>2,4</sup> Gerald H. Thomsen,<sup>5,6</sup> and Hiroaki Kiyokawa<sup>1,2,3</sup>

<sup>1</sup>Department of Molecular Pharmacology and Biological Chemistry and <sup>2</sup>Robert H. Lurie Comprehensive Cancer Center, Feinberg School of Medicine, Northwestern University, Chicago, IL 60611

<sup>3</sup>Department of Biochemistry and Molecular Genetics, College of Medicine, University of Illinois, Chicago, IL 60607

<sup>4</sup>Department of Medicine, Evanston Northwestern Healthcare Research Institute, Evanston, IL 60201

<sup>5</sup>Department of Biochemistry and Cell Biology and <sup>6</sup>Center for Developmental Genetics, Stony Brook University, Stony Brook, NY 11794

**A**ctivation of the anaphase-promoting complex/cyclosome (APC/C) by Cdc20 is critical for the metaphase-anaphase transition. APC/C-Cdc20 is required for polyubiquitination and degradation of securin and cyclin B at anaphase onset. The spindle assembly checkpoint delays APC/C-Cdc20 activation until all kinetochores attach to mitotic spindles. In this study, we demonstrate that a HECT (homologous to the E6-AP carboxyl terminus) ubiquitin ligase, Smurf2, is required for the spindle checkpoint. Smurf2 localizes to the centrosome, mitotic midbody, and centromeres. Smurf2 depletion or the expression of a catalytically inactive

Smurf2 results in misaligned and lagging chromosomes, premature anaphase onset, and defective cytokinesis. Smurf2 inactivation prevents nocodazole-treated cells from accumulating cyclin B and securin and prometaphase arrest. The silencing of Cdc20 in Smurf2-depleted cells restores mitotic accumulation of cyclin B and securin. Smurf2 depletion results in enhanced polyubiquitination and degradation of Mad2, a critical checkpoint effector. Mad2 is mislocalized in Smurf2-depleted cells, suggesting that Smurf2 regulates the localization and stability of Mad2. These data indicate that Smurf2 is a novel mitotic regulator.

## Introduction

Mitotic progression is controlled by spatiotemporal changes in protein modifications, i.e., phosphorylation mediated by several mitotic kinases and ubiquitination mediated by multiple E3 ubiquitin ligases (Nurse, 2000; Gutierrez and Ronai, 2006; Malumbres and Barbacid, 2007). The E3 activity of the anaphase-promoting complex/cyclosome (APC/C), which is sequentially activated by Cdc20 and Cdh1, plays a central role in coordinating mitotic progression by targeting multiple mitotic regulators to polyubiquitination-dependent degradation (Nasmyth, 2005; Peters, 2006). APC/C-Cdc20 is required for degradation of securin and cyclin B at anaphase onset. Securin keeps separase from inducing proteolysis of cohesin, which holds a pair of sister chromatids together during early mitosis. The spindle assembly checkpoint delays APC/C-Cdc20 activation until all chromosomes become aligned at the metaphase plate with

proper spindle attachment (Musacchio and Hardwick, 2002; Bharadwaj and Yu, 2004). Perturbation of this checkpoint results in chromosome missegregation and aneuploidy. The spindle assembly checkpoint depends on multiprotein complexes including Mad2, BubR1, and Bub3, known as the mitotic checkpoint complex (MCC). The physical assembly of MCC and its target Cdc20 is regulated according to the status of the spindle-kinetochore attachment and tension. Among the MCC components, Mad2 undergoes very dynamic changes in its conformation and localization (Howell et al., 2004). Current models suggest that unattached kinetochores are associated stably with Mad1 and Bub1, whereas Mad2 in differential conformations dynamically interacts with kinetochore-bound Mad1 and cytoplasmic Cdc20 (Nasmyth, 2005; Yu, 2006), which keeps APC/C-Cdc20 inactive in the presence of unattached or untensed kinetochores.

Correspondence to Hiroaki Kiyokawa: Kiyokawa@northwestern.edu

Abbreviations used in this paper: ACA, anticentromere antibody; APC/C, anaphase-promoting complex/cyclosome; dsRNA, double-stranded RNA; HECT, homologous to the E6-AP carboxyl terminus; MCC, mitotic checkpoint complex.

The online version of this article contains supplemental material.

© 2008 Osmundson et al. This article is distributed under the terms of an Attribution-Noncommercial-Share Alike-No Mirror Sites license for the first six months after the publication date (see <http://www.jcb.org/misc/terms.shtml>). After six months it is available under a Creative Commons License (Attribution-Noncommercial-Share Alike 3.0 Unported license, as described at <http://creativecommons.org/licenses/by-nc-sa/3.0/>).

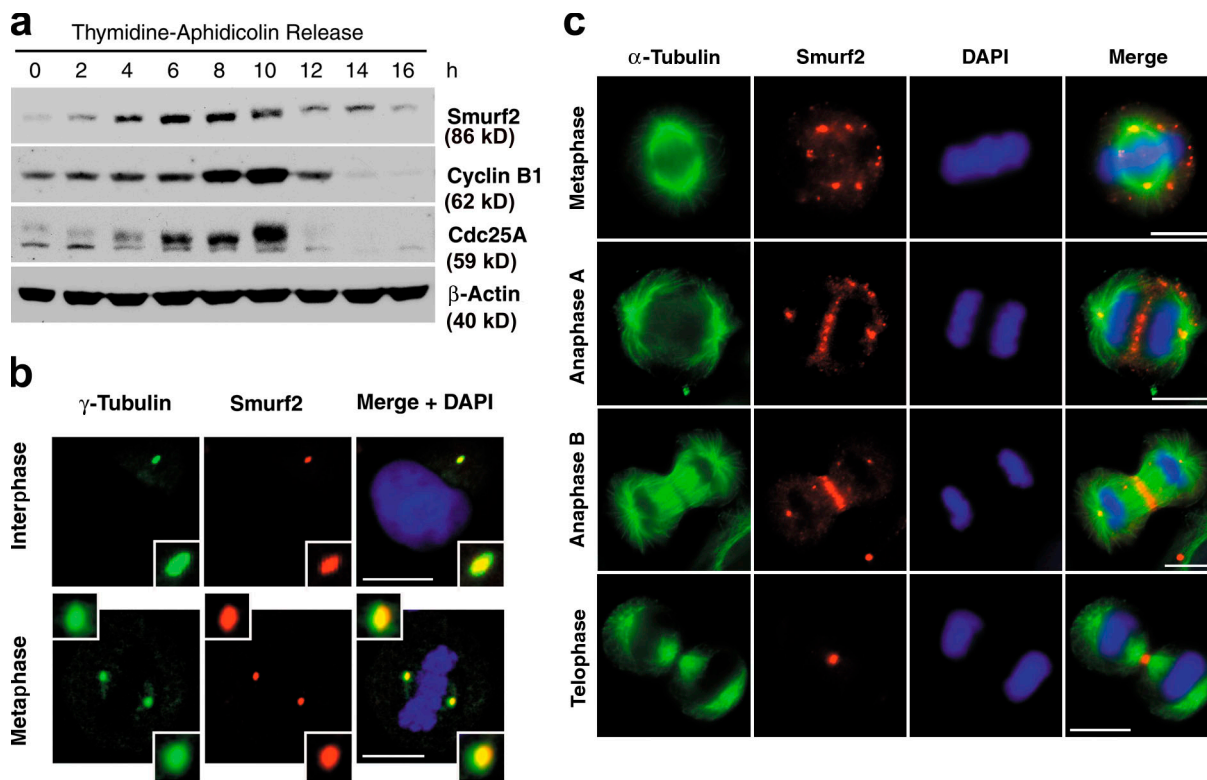


**Figure 1. Smurf2 is a cell cycle-regulated protein localizing specifically in the centrosome, mitotic midzone, and midbody.** (a) HeLa cells were synchronized by a double-thymidine protocol. At the indicated hours after release from the block, cells were analyzed by immunoblotting for the proteins shown. (b) Immunofluorescence microscopy for  $\gamma$ -tubulin (green) and Smurf2 (red) in HeLa cells at interphase and metaphase. Polyclonal anti-Smurf2 antibody was used for Smurf2 staining. DAPI was used to stain chromosomal DNA (blue). The close-up images are shown with threefold higher magnification. (c) Immunofluorescent staining for  $\alpha$ -tubulin (green) and Smurf2 (red) in human mammary epithelial MCF-10A cells during mitosis. Bars, 10  $\mu$ m.

Consistent with the key function of Mad2 in the spindle assembly checkpoint, recent studies using transgenic and knockout mouse models suggest that optimal control of Mad2 is critical for genomic stability and tumor suppression (Michel et al., 2001; Sotillo et al., 2007). Mad2 transcription is known to be regulated in E2F- and Myc-dependent manners (Hernando et al., 2004; Menssen et al., 2007). Although phosphorylation of Mad2 controls the association of Mad2 with Mad1 and APC/C-Cdc20 (Wassmann et al., 2003), it remains obscure whether Mad2 undergoes other posttranslational regulation. In this study, we demonstrate that a HECT (homologous to the E6-AP carboxyl terminus) family E3 ubiquitin ligase, Smurf2, plays an essential role in the spindle assembly checkpoint, regulating the stability and localization of Mad2. Smurf2 has been known as a negative regulator of the TGF- $\beta$  signaling pathway, targeting receptors and signaling proteins (Kavsak et al., 2000; Bonni et al., 2001; Stroschein et al., 2001; Moren et al., 2005). Previous studies demonstrated that Smurf2 targets TGF- $\beta$  receptors to proteasomal degradation (Kavsak et al., 2000; Di Guglielmo et al., 2003). Smurf2 also has been shown to ubiquitinate Smad2, the TGF- $\beta$ -related transcriptional cofactor SnoN (Bonni et al., 2001), the GTPase Rap1B (Schwamborn et al., 2007), the RING-H2 protein RNF11 (Subramaniam et al., 2003), the Runt domain transcription factors Runx2 and Runx3 (Jin et al., 2004; Kaneki et al., 2006), and  $\beta$ -catenin (Han et al., 2006). Although diverse transcriptional control by Smurf2-mediated ubiquitination is well documented, it was unknown that the expression and local-

ization of Smurf2 are cell cycle regulated, and the E3 activity of Smurf2 is critical for the spindle assembly checkpoint. The novel function of Smurf2 suggests that a network of ubiquitination machinery maintains the genomic stability during mitotic progression.

## Results

### Smurf2 is required for mitotic control during unperturbed cell cycle progression

Pub1p, a fission yeast HECT family E3 ligase, regulates G<sub>2</sub>/M cell cycle progression by ubiquitinating Cdc25p (Nefsky and Beach, 1996). The mammalian HECT family includes Smurf1, Smurf2, AIP4/Itch, and Nedd4 (Kee and Huibregtse, 2007). Our recent study on the TGF- $\beta$  regulation of Cdc25A ubiquitination (Ray et al., 2005) led us to examine whether Smurf proteins, which are known to modulate TGF- $\beta$  signaling (Zhu et al., 1999; Kavsak et al., 2000), were involved in mitotic regulation. We first examined the levels of Smurf2 protein in HeLa cells synchronized by a thymidine-aphidicolin protocol (Fig. 1 a). The expression of Smurf2 protein was highest 6–8 h after release, which slightly preceded the peaks of cyclin B1 and Cdc25A expression around G<sub>2</sub>/M transition. Smurf1 expression was constant throughout the cell cycle (unpublished data). Thus, Smurf2 is a cell cycle-regulated protein that accumulates during late G<sub>2</sub> through early mitosis. We then examined the subcellular localization of Smurf2, which revealed concentrated localization of

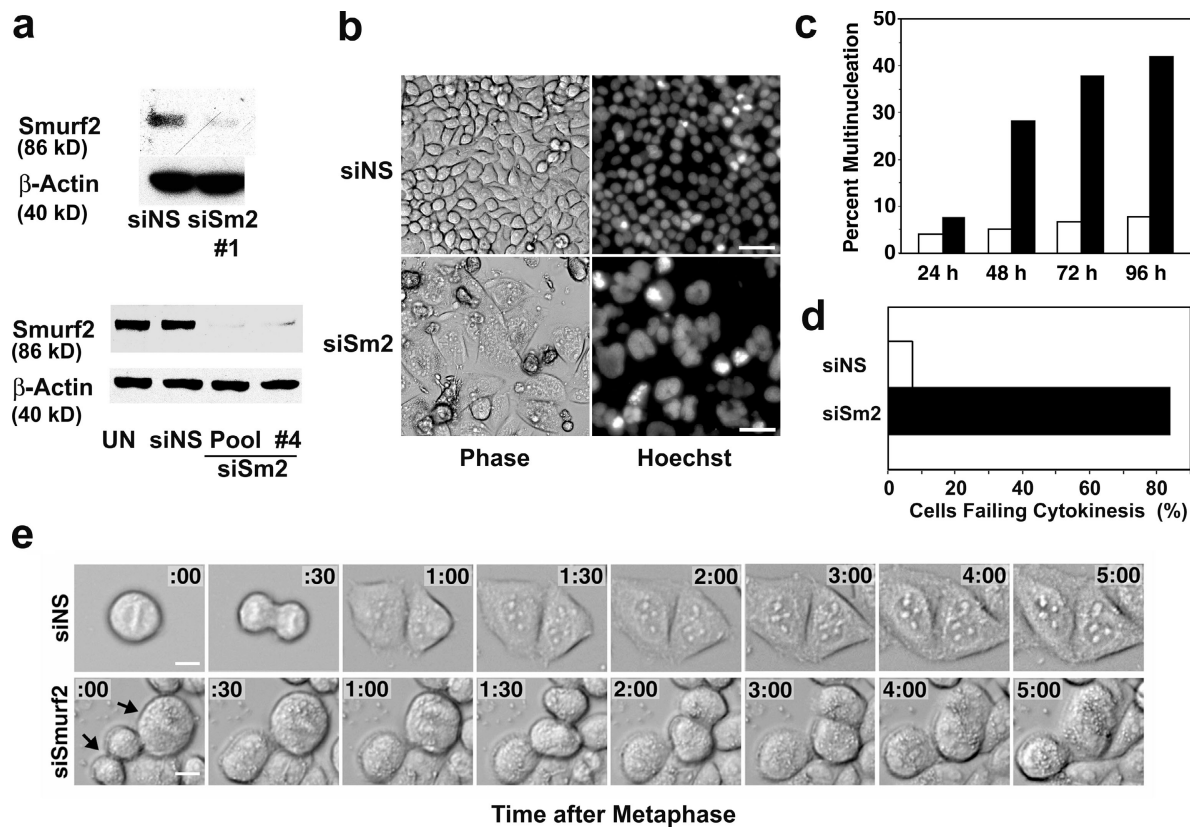


**Figure 2. Smurf2 silencing inhibits mitotic progression and cytokinesis.** (a) Smurf2 levels determined by immunoblotting in HeLa cells (top) and U2OS cells (bottom) 48 h after transfection with anti-Smurf2 siRNA (siSm2) or nonspecific dsRNA (siNS). UN, untransfected control. (b) Morphology of multinucleated HeLa cells 48 h after transfection with siRNA #1. Hoechst was used for DNA staining. (c) Percentages of multinucleated cells in HeLa cultures at the indicated hours after transfection with siNS (open bars) or Smurf2 siRNA #1 (shaded bars). At least 300 cells were counted per time point per cohort. Mean of data from two independent experiments are shown. See Fig. S2 a (available at <http://www.jcb.org/cgi/content/full/jcb.200801049/DC1>) for raw data from the individual experiments. (d) Percentages of cells that failed cytokinesis in siNS- or siSm2-transfected HeLa cultures quantified from the time-lapse microscopy. At least 65 mitotic cells per cohort (siNS vs. siSm2) were analyzed for the progression of cytokinesis. (e) Representative time-lapse pictures of siSm2-transfected HeLa cells that showed impaired mitotic progression and failed cytokinesis. Bars: (b) 50  $\mu$ m; (e) 10  $\mu$ m.

Smurf2 at centrosomes in HeLa cells (Fig. 1 b). The specificity of Smurf2 polyclonal antibody used for immunofluorescence microscopy was verified by immunoblotting with Smurf2-depleted cells (Fig. S1 a, available at <http://www.jcb.org/cgi/content/full/jcb.200801049/DC1>). Smurf2 localized at perinuclear centrosomes during interphase as well as at centrosomes aligned bipolarly in metaphase cells, demonstrating colocalization with a centrosomal marker,  $\gamma$ -tubulin. Similar centrosomal localization of Smurf2 was observed in HeLa cells using Smurf2 monoclonal antibody and pericentrin antibody, another centrosomal marker, as well as in U2OS cells transfected with Flag-tagged Smurf2 (Fig. S1, b and c). We then examined Smurf2 localization in MCF-10A cells undergoing mitosis and cytokinesis in which the protein exhibited a dynamic relocation pattern. Smurf2 localized predominantly at centrosomes during metaphase, whereas focal signals for Smurf2 were also observed in noncentrosomal structures in the cytoplasm (Fig. 1 c). During anaphase, a portion of Smurf2 apparently relocated to the center of the spindle midzone, which is rich in microtubules stained with  $\alpha$ -tubulin antibody. During telophase, Smurf2 was found concentrated at the midbody in the intercellular bridge. Similar Smurf2 relocation during mitosis was observed in HeLa cells (unpublished data).

To examine whether Smurf2 plays a role in mitotic progression, we examined the effects of siRNA-mediated Smurf2 depletion on divisions of cultured cell lines. We designed several siRNAs based on the coding region of human Smurf2 mRNA and tested the silencing efficiencies. Of them, siRNAs #1 and #4 as well as a pool of four siRNAs showed marked down-regulation of Smurf2 protein in transfected cells (Fig. 2 a). Morphological examinations readily detected several multinucleated HeLa cells transfected with Smurf2 siRNA #1 but not with control double-stranded RNAs (dsRNAs; Fig. 2, b and c). Similar multinucleation was observed in cells transfected with siRNA #4 or the pooled anti-Smurf2 siRNAs, whereas other siRNAs with poor knockdown efficiencies had no effect on nuclear morphology. Time-lapse microscopy demonstrated that most control HeLa cells initiated cytokinesis shortly after metaphase and did not revert from cytokinesis during 5 h of monitoring (Fig. 2 e and Video 1, available at <http://www.jcb.org/cgi/content/full/jcb.200801049/DC1>). In contrast, a majority of Smurf2 siRNA-transfected cells did not display well-defined cytokinesis after mitotic rounding up (time 0). Although formation of the cleavage furrow was observed,  $\sim$ 84% of cells with Smurf2 depletion failed cytokinesis, leading to a binucleated state (Fig. 2 d). Similar multinucleation phenotypes were observed in U2OS and

MCF-10A cells with Smurf2 depletion (unpublished data). Thus, Smurf2 is required for successful cytokinesis.

To explore the mechanism of mitotic failure in Smurf2-depleted cells, we first examined the parameters of chromosomal alignment and segregation because cells defective in the regulation of these events, e.g., depletion of Mad2 or USP44, demonstrate similar mitotic phenotypes (Michel et al., 2004; Stegmeier et al., 2007). We first examined the morphology of mitotic control and Smurf2-depleted HeLa cells during mitosis by staining for the microtubule marker  $\alpha$ -tubulin, Smurf2, and chromosomal DNA (Fig. S2 b, available at <http://www.jcb.org/cgi/content/full/jcb.200801049/DC1>). Of a total of >600 cells examined per group, 7.3% and 8.0% in control and Smurf2-depleted cells, respectively, displayed characteristics of mitosis (i.e., chromatin condensation and formation of mitotic spindles). Although 4.7% of control cells were found to be in metaphase, only 1.9% of Smurf2-depleted cells exhibited typical metaphase morphology with aligned chromosomes. The decrease in the metaphase population suggested that Smurf2 depletion might affect mitotic progression. To further assess the impact of Smurf2 depletion on chromosomal dynamics during mitotic progression, we depleted Smurf2 in HeLa cells stably expressing a GFP–histone H2B fusion protein (GFP-H2B). Cells were then monitored for chromosome movement by time-lapse microscopy, which readily showed that Smurf2-depleted cells initiated anaphase in the presence of misaligned chromosomes. Over 75% of Smurf2-depleted cells exhibited misaligned chromosomes or failed to form a metaphase plate during monitored metaphase–anaphase transition (Fig. 3, a and b; and Video 2). During anaphase, most Smurf2-depleted cells showed defective segregation such as lagging chromosomes or no appreciable chromosome segregation (Fig. 3, c and d). In contrast, <10% of control cells exhibited such defects during mitosis. We also measured the interval between nuclear envelope breakdown and the onset of anaphase, focusing on cells that displayed discernable elements of chromatin segregation. In control cultures, the median interval was  $\sim$ 55 min, whereas that in Smurf2-depleted cultures was  $\sim$ 23 min (Fig. 3, e and f; and Video 3). These data indicate that Smurf2 depletion leads to premature anaphase onset together with chromosomal alignment and segregation defects. Thus, Smurf2 seems to play a significant role in the temporal control of the metaphase–anaphase transition, a process normally regulated by the spindle assembly checkpoint.

#### **Smurf2 regulates the spindle assembly checkpoint**

Defective chromosome alignment/segregation and premature anaphase onset in Smurf2-depleted cells are reminiscent of the phenotypes of impaired spindle assembly checkpoint. To examine whether Smurf2 is involved in the checkpoint, cells progressing synchronously through  $G_2$  toward M were treated with the microtubule polymerization inhibitor nocodazole. For examinations of Smurf2 localization, cells were fixed as they progressed into pro-metaphase arrest (Fig. 4 a). Interestingly, Smurf2 localized in a focal fashion and was closely associated with the immunoreactivities against human anticentromere antibodies (ACAs), which recognize several centromere proteins (Earnshaw et al., 1986).

The localization of Smurf2 at centromeres was observed only transiently in cells undergoing nocodazole-induced arrest at pro-metaphase. This localization pattern is consistent with a putative role for Smurf2 in the spindle assembly checkpoint. We then determined cellular levels of mitosis regulatory proteins in Smurf2-depleted and control cells synchronously progressing into mitosis in the presence of nocodazole (Fig. 4 b). Cellular levels of Smurf2 and the APC/C-Cdc20 substrates securin, cyclin B1, and aurora B (Fang et al., 1999) accumulated as control cells progressed through the  $G_2/M$  transition 8–10 h after release from the thymidine block. Cyclin A2 was markedly down-regulated during nocodazole-induced prometaphase arrest as expected (Fry and Yamano, 2006). Strikingly, securin, cyclin B1, and aurora B failed to accumulate in Smurf2-depleted cells. In contrast, Smurf2 depletion affected minimally or only modestly the levels of Emi1, cyclin A2, and the APC/C-Cdh1 substrates Plk1 and Cdc20. These proteins are not direct targets of APC/C-Cdc20, whereas cyclin B1, securin, and aurora B are well-characterized substrates. These data suggest that Smurf2 depletion results in premature activation of APC/C-Cdc20. Flow cytometry further demonstrated that control cells were arrested with 4N DNA content 14 h after release from the thymidine block, whereas 17% of Smurf2-depleted cells had 8N DNA, which is consistent with binucleation (Fig. 4 c). 26 h after release, 63% of Smurf2-depleted cells exhibited 8N DNA. These data suggest that Smurf2 depletion resulted in continued cell cycle progression in the presence of nocodazole without successful cytokinesis. To confirm that Smurf2 depletion permitted inappropriate APC/C-Cdc20 activity in the presence of nocodazole, we attempted to silence Cdc20 in Smurf2-depleted cells (Fig. 4 d). siRNA-mediated codepletion of Cdc20 and Smurf2 resulted in restored mitotic accumulation of cyclin B1 and securin (but not Mad2; Fig. 4 d, fourth row) in synchronized cultures of nocodazole-treated HeLa cells. Aurora B is also up-regulated modestly by the codepletion. Importantly, the addition of Cdc20 siRNA did not significantly affect the silencing efficacy of the Smurf2 siRNA or the levels of cyclin A2 and Plk1. These data suggest that Smurf2 is required for the spindle assembly checkpoint-mediated inhibition of APC/C-Cdc20 and mitotic accumulation of securin and cyclin B1.

#### **Smurf2 is required for stability and proper localization of Mad2**

When the spindle assembly checkpoint is activated, e.g., by nocodazole, Mad2 localizes in multiprotein complexes at unattached or untensed kinetochores, including Mad1 and Bub1 (Bharadwaj and Yu, 2004). Cells lacking Mad2 demonstrate a severely compromised spindle assembly checkpoint (Michel et al., 2004). Immunoblotting demonstrated that Mad2 was markedly down-regulated in Smurf2-depleted cells, whereas Mad2 levels were relatively constant during cell cycle progression of control cells (Fig. 4, b and d). Immunofluorescence microscopy also confirmed that no specific localization of Mad2 was detected at centromeres of Smurf2-depleted cells (Fig. 4 e), whereas localization of BubR1 at centromeres was unaffected (Fig. 4 f). Moreover, Smurf2 depletion down-regulated not only endogenous Mad2 but also transfected Mad2 in asynchronous HeLa

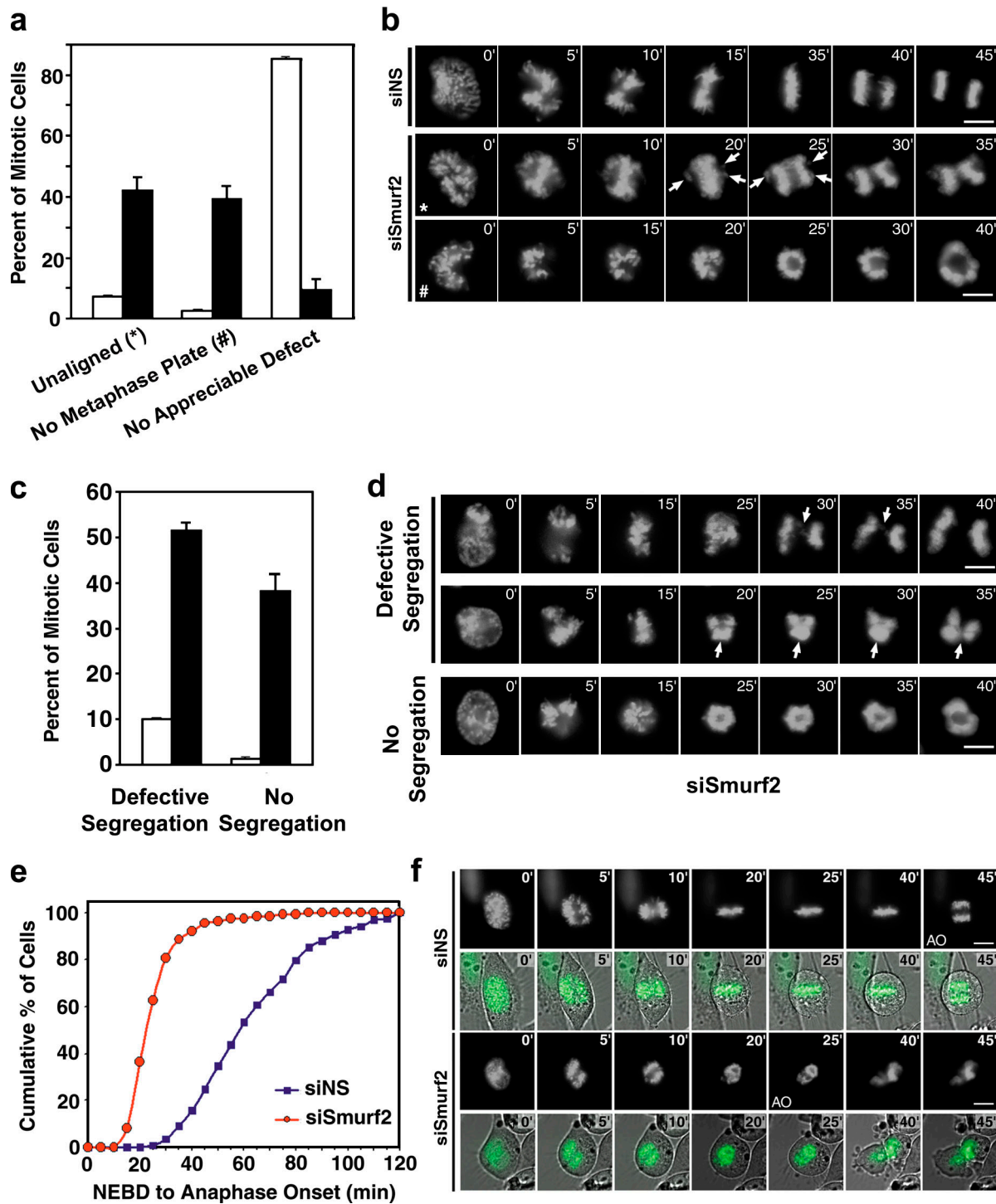


**Figure 3. Smurf2 silencing leads to chromosomal misalignment at metaphase and premature onset of anaphase with defective chromosome segregation.** HeLa cells stably expressing GFP-H2B were transfected with Smurf2 siRNA #1, and chromosomal movement was monitored 24–25 h after transfection by time-lapse fluorescence microscopy. Quantified data are representative of at least two independent experiments. (a) Defects in chromosomal alignment in Smurf2-depleted cells at metaphase. Metaphase defects in cells transfected with Smurf2 siRNA (shaded bars) or nonspecific dsRNA (siNS, open bars) were categorized into the two indicated groups. (b) Unaligned chromosomes (\*) and lack of metaphase plates (#) during mitosis with Smurf2 depletion. Arrowheads denote lagging chromosomes. (c) Chromosomal segregation defects in GFP-H2B HeLa cells transfected with Smurf2 siRNA (shaded bars) or nonspecific dsRNA (open bars) at anaphase. (a and c) Data are means  $\pm$  SEM (error bars) from three independent experiments. (d) Lagging chromosomes (arrowheads, top row), major segregation defects (arrowheads, middle row), and lack of segregation in GFP-H2B HeLa cells with Smurf2 depletion. (e) Premature anaphase onset in Smurf2-depleted cells. The metaphase–anaphase transition of GFP-H2B HeLa cells was monitored by time-lapse microscopy, and the time from nuclear envelope breakdown (NEBD) until anaphase onset was determined. (f) Representative pictures of the metaphase–anaphase transition. AO, anaphase onset. Bars, 10  $\mu$ m.

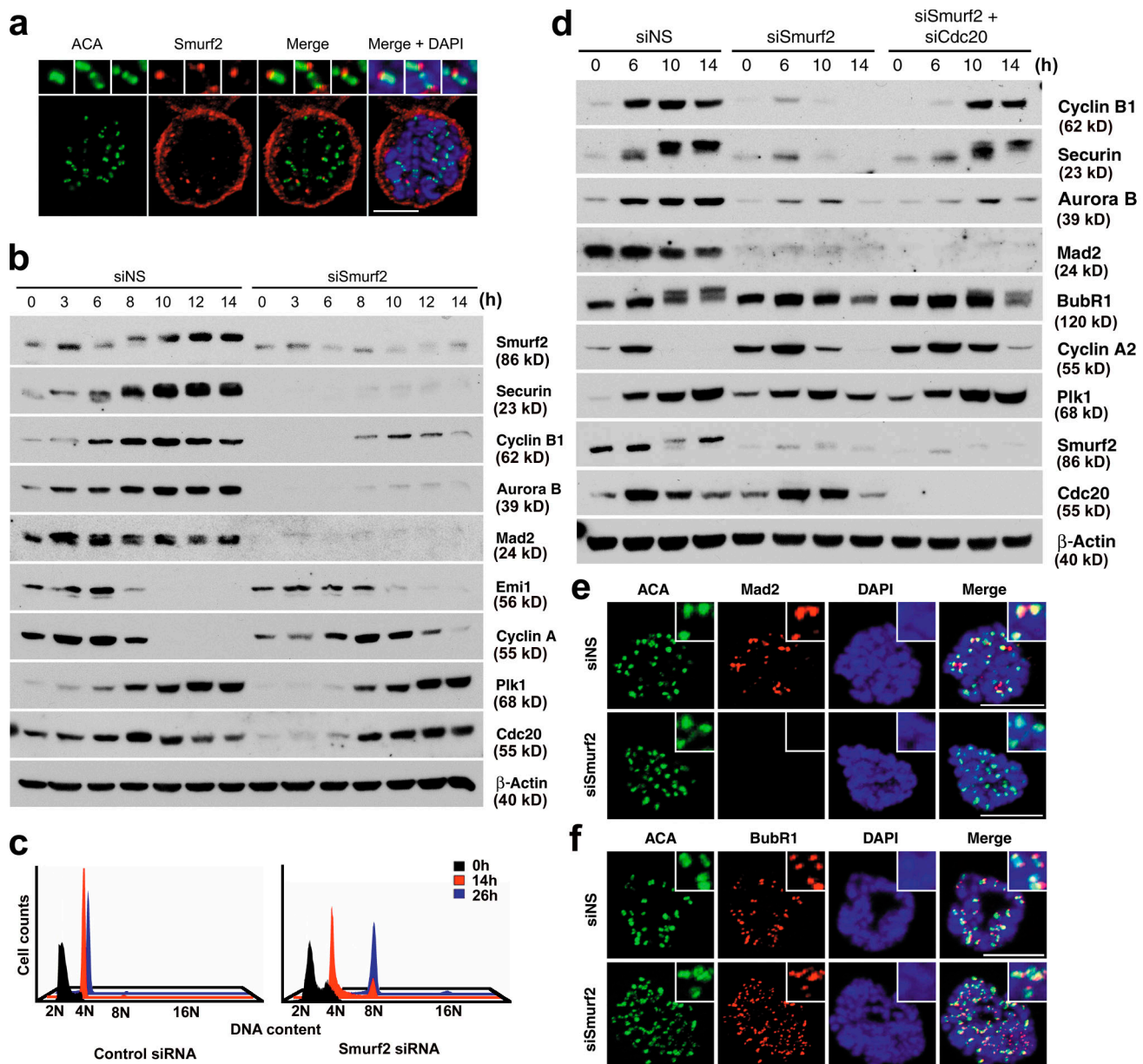


**Figure 4. Smurf2 is a novel regulator of the spindle assembly checkpoint.** (a) Smurf2 localizes at centromeres when the spindle checkpoint is active. HeLa cells were synchronized by a double-thymidine protocol (see Materials and methods). Cells were then released into a fresh medium (time 0), and 3 h later nocodazole was added. Immunofluorescence microscopy after staining with ACA, anti-Smurf2 antibody, and DAPI for DNA. Cells were fixed 8.5 h after release from the thymidine in the presence of nocodazole. (b) Smurf2 depletion results in failed accumulation of APC/C-Cdc20 substrates during nocodazole-induced metaphase arrest. Immunoblotting was performed for mitotic regulators in HeLa cells transfected with Smurf2 siRNA #1 or nonspecific dsRNA [siNS]. After release from the thymidine block, cells were incubated for the indicated hours in the presence of nocodazole. (c) Smurf2-depleted cells override nocodazole-induced spindle assembly checkpoint, resulting in tetraploidy. Control (siNS) and Smurf2-depleted cells were fixed at the indicated times and subjected to flow cytometry. (d) Cosilencing of Cdc20 restores mitotic accumulation of cyclin B1 and securin in Smurf2-depleted HeLa cells. Cells were synchronized and released into nocodazole-containing medium as described in b. (e and f) Smurf2 depletion results in loss of Mad2 from centromeres, whereas centromere localization of BubR1 is unaffected. Cells were fixed 8.5 h after release from the thymidine in the presence of nocodazole, and immunofluorescence microscopy was performed. (a, e, and f) The close-up images are shown with threefold higher magnification. Bars, 10  $\mu$ m.

cells (Fig. S3 a, available at <http://www.jcb.org/cgi/content/full/jcb.200801049/DC1>). Mad2 down-regulation by Smurf2 depletion was confirmed in U2OS cells using Smurf2 siRNA #1 and #4 as well as pooled siRNAs (Fig. S3 b), suggesting that this is not an off-target effect of siRNAs. We then examined whether Smurf2 siRNA affected Mad2 mRNA levels (Fig. 5 a). Despite the rapid decline of Mad2 protein levels, Mad2 mRNA levels were essentially unaltered in Smurf2-depleted cells, indicating a posttranscriptional mechanism.

We suspected that Mad2 levels may be determined by ubiquitin-mediated proteasomal degradation, like many other cell cycle regulators. To examine whether Mad2 is ubiquitinated, Mad2 was immunoprecipitated from Smurf2-depleted or control HeLa cells treated with the proteasomal inhibitor MG132 followed by immunoblotting for ubiquitin (Fig. 5 b). Smurf2 depletion robustly increased polyubiquitinated forms of Mad2, and proteasomal inhibition

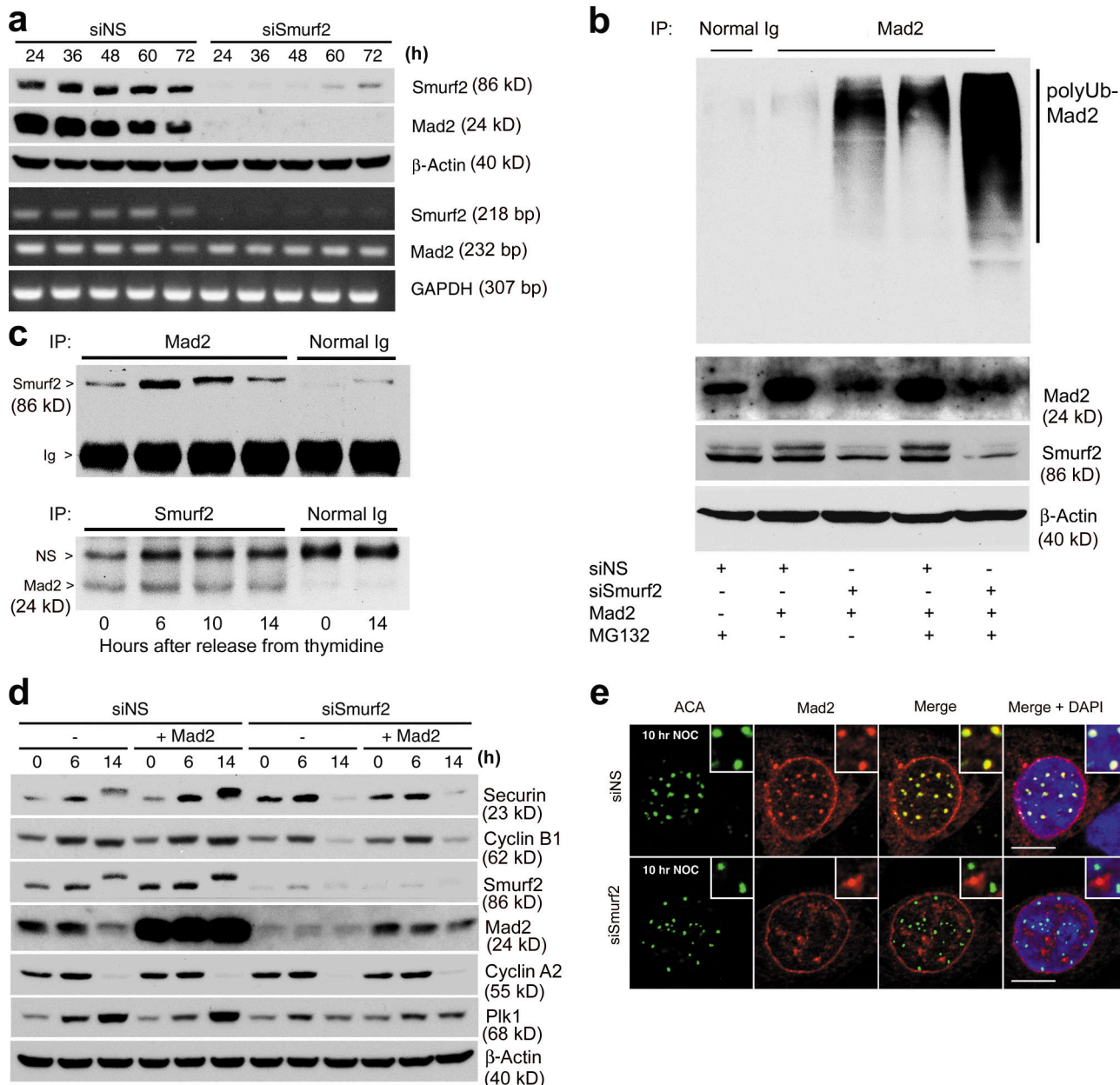


**Figure 5. Smurf2 is required for stability and functional localization of Mad2.** (a) Smurf2 silencing rapidly down-regulates Mad2 protein but not mRNA. HeLa cells in asynchronous culture were transfected with Smurf2 siRNA or nonspecific dsRNAs (siNS) and harvested at the indicated times after transfection for Western blotting and RT-PCR. (b) Smurf2 silencing results in increased polyubiquitination of Mad2 followed by proteasomal degradation. HeLa cells were transfected with a Mad2 expression plasmid and Smurf2 siRNA #1 or control dsRNA. Cells were then treated with 2  $\mu$ M MG132 for 4 h and analyzed by immunoprecipitation (IP) with Mad2 antibody followed by Western blotting using the indicated antibodies. (c) Smurf2 physically interacts with Mad2. Untransfected HeLa cells were released from synchronization at S phase with double-thymidine treatment and were harvested at the indicated times for immunoprecipitation followed by Western blotting. Ig, Ig heavy chain; NS, nonspecific band. (d) Ectopic expression of Mad2 is unable to restore the spindle assembly checkpoint in Smurf2-depleted cells. Western blotting for mitotic regulators in HeLa cells transfected with the indicated plasmid and siRNA. Cells were synchronized with thymidine treatment, released into a nocodazole-containing medium, and harvested at the indicated times after release (see Fig. 4 b and Materials and methods). (e) Ectopically expressed Mad2 localizes at centromeres in nocodazole-treated control cells but not in Smurf2-depleted cells. Immunofluorescence microscopy with anti-Mad2 and ACAs 10 h after release from the thymidine block. The close-up images are shown with threefold higher magnifications. Bars, 10  $\mu$ m.

by MG132 further accumulated polyubiquitinated Mad2. We also found that Smurf2 physically associates with Mad2. Endogenous Smurf2 and Mad2 coimmunoprecipitated with each other from extracts of untransfected HeLa cells that progressed from S phase into mitosis (Fig. 5 c, and see Fig. S4 for controls). These data suggest that Smurf2 normally protects Mad2 from polyubiquitination-dependent degradation.

We then examined whether the forced expression of Mad2 was sufficient to restore the spindle assembly checkpoint in Smurf2-depleted cells. Transfection of a Mad2 expression plasmid resulted in marked overexpression of Mad2 in cells without Smurf2 depletion, which did not significantly affect the expression of securin, cyclin B1, or other mitotic regulators during synchronous progression into nocodazole-induced arrest (Fig. 5 d).

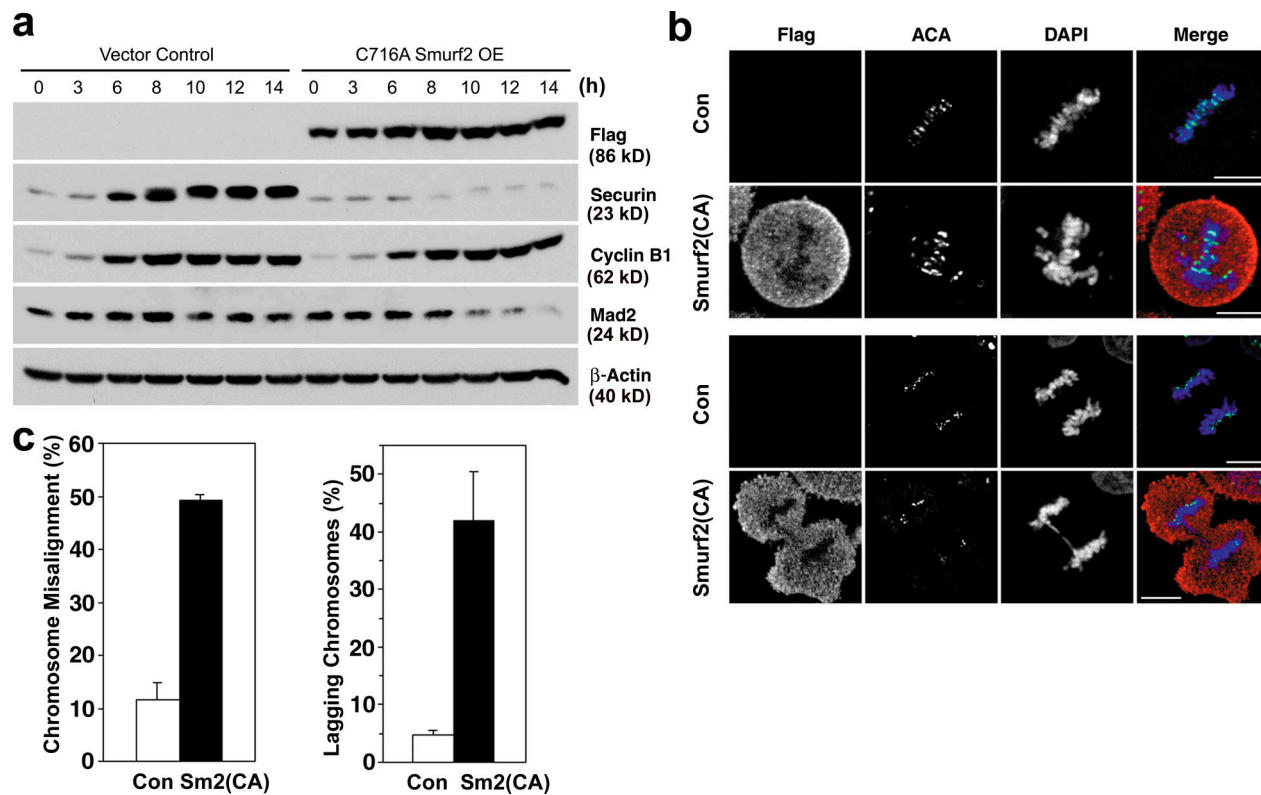


**Figure 6. Expression of a catalytically inactive Smurf2 impairs the spindle assembly checkpoint with Mad2 destabilization.** (a) Immunoblotting for mitotic regulators in HeLa cells transfected with Flag-tagged Smurf2(C716A) or a control plasmid. Cells were synchronized at S phase with thymidine treatment, released into a nocodazole-containing medium, and harvested after incubation at the indicated times after release (see Materials and methods). OE, overexpression. (b) Chromosomal misalignment at metaphase and lagging chromosomes at anaphase observed in cells expressing Smurf2(C716A). Immunofluorescence microscopy of cells stained with anti-Flag antibody for exogenously expressed Smurf2, ACA, and DAPI. Cells were harvested 8.5 h after release from the thymidine block. The second row shows misaligned chromosomes at metaphase, and the bottom row shows lagging chromosomes at anaphase in cells expressing Smurf2(C716A). Bars, 10  $\mu$ m. (c) Percentages of cells with chromosomal defects in control cultures (open bars) and Smurf2(C716A)-transfected cultures (shaded bars). Data are means  $\pm$  SEM (error bars) from three independent experiments.

In Smurf2-depleted cells, transfection of Mad2 resulted in accumulation of Mad2 to levels comparable with mock-transfected control cells. However, these cells exhibited almost undetectable levels of securin and cyclin B1, indicating that ectopic expression of Mad2 was insufficient to restore the checkpoint. Cyclin A2, which is known to be degraded even during spindle assembly checkpoint activation (Fry and Yamano, 2006), was nearly undetectable in nocodazole-treated cells of all cohorts. Apparently, the lack of phenotypic rescue was associated with mislocalization of exogenously expressed Mad2 because most Mad2 immunoreactivities of nocodazole-treated cells did not colocalize with the signals from ACAs (Fig. 5 e). The mean intensity of Mad2 signals normalized by ACA signals in a cell expressing exogenous Mad2 in the presence of siSmurf2 was 74% lower than that in a cell expressing exogenous Mad2 in the presence of siNS ( $3.208 \pm 0.217$  vs.  $0.823 \pm 0.068$ , mean  $\pm$  SEM, from centromeres examined in eight cells per group). These data suggest that Smurf2 may regulate not only the stability but also the localization of Mad2.

We next examined whether the E3 ligase activity of Smurf2 is important for its function to control the spindle assembly checkpoint. The cysteine-716 residue of Smurf2 is critical for its E3 ligase activity because Smurf2(C716A) protein is catalytically inactive (Kavsak et al., 2000). Thus, we transfected

HeLa cells with an expression plasmid for Smurf2(C716A) and synchronized them at early S phase with double-thymidine treatments (Fig. 6 a). Cells were then released into a nocodazole-containing medium. Immunoblotting showed that cells transfected with Smurf2(C716A) failed to accumulate securin with significant reduction in Mad2 levels. Interestingly, cyclin B1 accumulation during G<sub>2</sub>/M progression was minimally affected, which is analogous to previous observations in *Mad2* heterozygous cells (Michel et al., 2004). In contrast, transfection with wild-type Smurf2 affected none of these proteins (Fig. S5, available at <http://www.jcb.org/cgi/content/full/jcb.200801049/DC1>). This finding is consistent with the effects of Smurf2 siRNA, suggesting that Smurf2(C716A) can act as a dominant-negative mutant. Furthermore, cells transfected with Smurf2(C716A) showed a significant increase in cells displaying misaligned chromosomes, lagging chromosomes during mitotic exit, and multinucleation (Fig. 6, b and c). These data suggest that the E3 ligase activity of Smurf2 is required for proper control of the spindle assembly checkpoint.

## Discussion

This study has revealed a novel function of the HECT E3 ligase Smurf2 in mitosis. During unperturbed mitotic progression,

Smurf2 dynamically relocates from the centrosome to the center of the anaphase spindle midzone and finally to the midbody in the intercellular bridge during cytokinesis. Smurf2 is also observed at unattached centromeres during spindle assembly checkpoint activation. Smurf2 depletion impairs the spindle assembly checkpoint, leading to increased misalignment and missegregation of chromosomes, premature anaphase onset, and defective cytokinesis. The function of Smurf2 in the spindle assembly checkpoint is mediated at least partly by the stability and localization of Mad2 because Smurf2 depletion results in enhanced polyubiquitination and rapid destabilization of Mad2 protein. Mad2 destabilization presumably leads to premature activation of APC/C-Cdc20, which is associated with impaired mitotic accumulation of the APC/C-Cdc20 substrates such as cyclin B1 and securin. The silencing of Cdc20 in Smurf2-depleted cells restores mitotic accumulation of these proteins, confirming the antagonistic function of Smurf2 against APC/C-Cdc20 activity. Ectopic expression of Mad2 is insufficient to restore the spindle assembly checkpoint in Smurf2-depleted cells, apparently because Mad2 mislocalizes in the absence of Smurf2. Collectively, Smurf2 is a novel regulator of the Mad2-dependent spindle assembly checkpoint.

Mad2 interaction with kinetochore-associated checkpoint proteins, such as Mad1 and Bub1, is required for the inhibition of APC/C-Cdc20 until the proper alignment of all mitotic spindles (Nasmyth, 2005; Yu, 2006). Mad2, together with BubR1 and Bub3, exhibits rapid movement on and off kinetochores, transiently interacting with Mad1- and Bub1-associated centromeres (Howell et al., 2004). This dynamic regulation of Mad2 is critical for the diffusible inhibitory signal against cytoplasmic APC/C-Cdc20. This study presents evidence that Smurf2 activity is required for the normal progression of mitosis as well as for spindle disruption-mediated mitotic arrest. Similarly, cells with Mad2 or BubR1 depletion show various mitotic defects (i.e., failure in chromosome segregation, premature anaphase onset, and cytokinesis defects; Taylor and McKeon, 1997; Gorbsky et al., 1998; Meraldi et al., 2004). Analogous phenotypes have been observed in cells with depletion of USP44, a deubiquitinating enzyme that counteracts disassembly of Mad2–Cdc20 complexes by removing ubiquitin from Cdc20 (Stegmeier et al., 2007). The binding of Mad2 to Cdc20 requires a substantial conformational change of Mad2, which Mad1 seems to facilitate at the kinetochore (Yu, 2006). Although it remains to be elucidated how Smurf2 regulates the stability and localization of Mad2, it is tempting to speculate that the E3 ligase activity of Smurf2 is involved in regulating Mad2 conformation. Smurf2 levels are highest before the metaphase–anaphase transition, when Smurf2 localizes predominantly at spindle poles/centrosomes. Mad2 also has been found at spindle poles before anaphase onset, possibly via microtubule-mediated transit between kinetochores and spindle poles (Howell et al., 2000; Shah et al., 2004). Depletion of Mad2 and BubR1 results in kinetochore-independent premature anaphase onset, whereas knockdown of other spindle checkpoint components (e.g., Bub3 and Bub1) impairs only kinetochore-dependent checkpoint function, not the timing of anaphase onset (Meraldi et al., 2004). Our data demonstrating premature anaphase onset in Smurf2-depleted cells support a

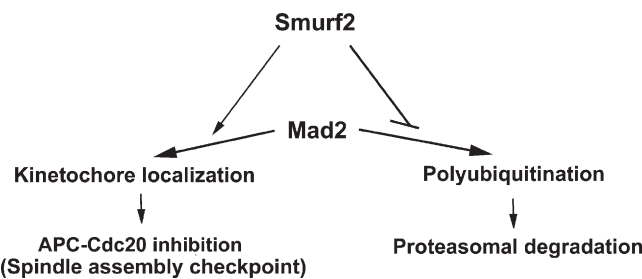


Figure 7. Putative roles of Smurf2 in regulation of the spindle assembly checkpoint.

hypothesis that a functional interaction of Smurf2 and Mad2 that occurs dynamically between spindle poles/centrosome and kinetochores may control the spindle assembly checkpoint. Of course, it is possible that Smurf2 plays multiple roles in mitosis and cytokinesis by affecting multiple downstream targets in addition to Mad2. A previous study showed that Smad2, 3, and 4 bind to microtubules in the absence of TGF- $\beta$ , colocalizing with tubulin at the bipolar spindle and midzone (Dong et al., 2000). These Smad proteins can function as a co-factor of multiple E3 ligases, including SCF (skp1-Cul1-F-box), APC/C, and Smurf2 (Fukuchi et al., 2001; Ogunjimi et al., 2005; Ray et al., 2005). Therefore, the cofactor Smad protein might complex with Smurf2 alongside microtubules and modulate Smurf2 activity.

Regulation upstream of the spindle checkpoint components has been understudied. The transcriptional control of Mad2 by E2F and Myc was recently identified (Hernando et al., 2004); however, it had been unknown whether cellular levels of Mad2 protein are regulated by ubiquitination. To our knowledge, this study is the first to demonstrate that Mad2 undergoes polyubiquitination and proteasomal degradation. The experiments using Smurf2 siRNA and Smurf2(C716A) showed that the E3 ligase activity of Smurf2 is required to prevent Mad2 from polyubiquitination and degradation (Fig. 7). Smurf2 physically associates with Mad2. Although Smurf2 is likely to affect the modification and/or conformation of Mad2 at close proximity, the precise mechanism remains to be determined. A hypothetical mechanism is that Smurf2 directly modifies Mad2 by mono-ubiquitination or Lys63-linked polyubiquitination (Haglund and Dikic, 2005), and such a modification somehow alters the conformation of Mad2 to a stable form and promotes its dynamic localization at kinetochores critical for surveillance of spindle integrity. For instance, the chromatin passenger complex protein survivin undergoes Lys63 polyubiquitination, which is required for centromere localization of this protein (Vong et al., 2005). When the level of active Smurf2 is low, Mad2 undergoes an alternative form of ubiquitination, presumably Lys48-linked polyubiquitination mediated by an undefined E3 ligase, and is recruited to proteasomal degradation. Another possibility is that Smurf2 plays an indirect role in the control of Mad2 stability. Smurf2 may antagonize the action of an unidentified E3 ligase required for proteasomal degradation of Mad2, possibly by ubiquitinating and destabilizing the E3 ligase. In this case, Smurf2 depletion would up-regulate the E3 ligase by stabilization, leading to enhanced Mad2 polyubiquitination and subsequent

proteasomal degradation. Further biochemical investigations are needed to evaluate these hypotheses regarding the Mad2 regulatory function of Smurf2.

## Materials and methods

### Antibodies

Monoclonal antibody against human Smurf2 has been described previously (Kavsak et al., 2000). Polyclonal Smurf2 antibody was purchased from Millipore. Antibodies against Mad2 and Cdc20 were purchased from Santa Cruz Biotechnology, Inc. Anti-aurora B antibody was obtained from BD Biosciences. Antibodies against  $\gamma$ -tubulin (GTU88),  $\alpha$ -tubulin (DM1A), BubR1 (8G1), and  $\beta$ -actin (AC-15) were purchased from Sigma-Aldrich. Antibodies against securin, Plk1, and Emi1 were purchased from Invitrogen. Anti-cyclin B1 (Ab-2) and -cyclin A2 (Ab-6) antibodies were purchased from Neomarkers. Anticentromere CREST autoantiserum was obtained from Immunovision. FITC-conjugated anti-rabbit Ig and Texas red-conjugated anti-human Ig were purchased from Vector Laboratories.

### Cell cultures

Human cervical carcinoma HeLa cells, osteosarcoma U2OS cells, and mammary epithelial MCF-10A cells were obtained from the American Type Culture Collection. HeLa and U2OS cells were cultured in Dulbecco's modified minimum essential medium supplemented with 10% fetal bovine serum. MCF-10A cells were cultured in Dulbecco's modified minimum essential medium/F12 medium supplemented with 5% heat-inactivated horse serum, 10  $\mu$ g/ml insulin, 0.5  $\mu$ g/ml hydrocortisone, and 20 ng/ml recombinant human EGF. For the stable expression of GFP-H2B, HeLa cells were transfected with pBOS-H2B-GFP (Invitrogen; stable cell line provided by C. Zou, Northwestern University, Evanston, IL). To synchronize cells with a double-thymidine protocol, cells were treated first with 2 mM thymidine for 18 h, washed once in PBS, and released into fresh media. 9 h later, thymidine was added to the culture medium to 2 mM, and incubation was continued for 15 h. Cells were then released into a fresh medium for synchronous progression of the cell cycle from early S phase. To closely examine cells progressing into mitosis and the integrity of the spindle assembly checkpoint, nocodazole was added into the medium 3 h after release from the second thymidine block to a concentration of 300 nM. In this scheme, cells started to arrest at prometaphase within 10 h after release from the second thymidine treatment. To silence Smurf2 and Cdc20 in synchronized cell cultures, cells were transfected with either control or Smurf2 siRNAs 5 h before the beginning of the first thymidine treatment and transfected with either control or Cdc20 siRNAs 2 h after the release of the first thymidine treatment. To determine cell cycle profiles, cells were fixed with ice-cold ethanol and stained with propidium iodide as described previously (Tsutsui et al., 1999). The sense sequences of the Smurf2 #1 and #4 siRNAs are 5'-GAUGAGAACACUCAUUUAUU-3' and 5'-CAAAGUGGAAUCAGCAUUUAUU-3', respectively. The SMARTpool siRNAs against Smurf2 and Cdc20 and the control dsRNAs were obtained from Thermo Fisher Scientific.

### Immunofluorescence and time-lapse microscopy

For subcellular localization analyses, cells were fixed with ice-cold methanol for at least 20 min. Alternatively, cells were initially fixed with 10% buffered formalin (Sigma-Aldrich) for 5 min and fixed with ice-cold methanol for 20 min. For centromeric localization of Smurf2 and other antigens, cells were prepermeabilized with PBS supplemented with 0.5% Triton X-100 and 1 mM MgCl<sub>2</sub> followed by fixation with 10% buffered formalin or, alternatively, fixation with ice-cold methanol as described above. Slide glasses with fixed cells were then washed with PBS, permeabilized with 0.2% Triton X-100 on ice for 5 min, and stained with primary antibodies at 4°C for 16 h. Washed slides were then incubated with fluorescence-conjugated secondary antibodies at 4°C for 1 h. Washed slides were shielded with coverglasses using Vectashield containing DAPI stain (Vector Laboratories) and subjected to microscopic analyses at 25°C. For microscopic studies, we used an inverted fluorescence microscope (Axiovert 200; Carl Zeiss, Inc.) with a 40 $\times$  NA 0.55 objective lens equipped with a Hg lamp (X-Cite 120; EXFO Photonic Solutions, Inc.). An AxioVision Digital Imaging System with a 3D deconvolution camera (Apotome and AxioCam MRm; Carl Zeiss, Inc.) was used for data acquisition and analyses as well as for time-lapse analyses of live cells. Time-lapse examinations of GFP-H2B-expressing HeLa cells for chromatin alignment and segregation and anaphase onset were performed as previously described (Rieder et al., 1994; Meraldi et al., 2004).

### Protein analyses

For immunoblotting or immunoprecipitation, cells were lysed by sonication in lysis buffer as described previously (Tsutsui et al., 1999). Densitometric analyses of chemiluminescence signal were performed using a 1D Scientific Imaging Systems version 3.6.1 (Kodak) and ScanMaker i800 (Microtek).

### Online supplemental material

Video 1 shows impaired mitotic progression, failed cytokinesis, and binucleation in Smurf2 siRNA (siSmurf2)-transfected HeLa cells demonstrated by time-lapse phase microscopy. Video 2 shows defective chromosomal alignment in Smurf2-depleted (siSmurf2) GFP-H2B HeLa cells at metaphase demonstrated by time-lapse fluorescence microscopy. Video 3 shows premature anaphase onset in Smurf2-depleted (siSmurf2) GFP-H2B HeLa cells demonstrated by time-lapse fluorescence microscopy. Fig. S1 shows centrosomal localization of endogenous and transfected Smurf2 examined by multiple antibodies. Fig. S2 shows multinucleation and misaligned chromosomes in HeLa cells with Smurf2 depletion. Fig. S3 shows down-regulation of endogenous and transfected Mad2 in cells with Smurf2 depletion. Fig. S4 shows control immunoblots for Fig. 5 c. Fig. S5 shows that overexpression of wild-type Smurf2 minimally affects levels of securin, cyclin B1, and Mad2. Online supplemental material is available at <http://www.jcb.org/cgi/content/full/jcb.200801049/DC1>.

We thank Brian Zwecker, Thomas O'Grady, Alba Santana, and Suchitra Prasad for technical help, Chaozhong Zou for reagents, and Toru Nakamura, Alisa Katzen, Pradip Raychaudhuri, Elena Pugacheva, Erica Golemis, Kenji Fukasawa, and the Northwestern Cancer Cell Biology group for helpful discussions.

This work was supported partly by the National Institutes of Health (grants CA112282, CA100204, and HD38085 to H. Kiyokawa and grants CA095221 and CA96986 to Q. Gao), the Department of Defense (grant DAMD17-01-1-0342 to Q. Gao), the American Cancer Society (grant RSG-03-048-01 to Q. Gao), and the Searle Leadership Fund and Zell Fund (grants to H. Kiyokawa).

Submitted: 9 January 2008

Accepted: 10 September 2008

## References

- Bharadwaj, R., and H. Yu. 2004. The spindle checkpoint, aneuploidy, and cancer. *Oncogene*. 23:2016–2027.
- Bonni, S., H.R. Wang, C.G. Causing, P. Kavsak, S.L. Stroschein, K. Luo, and J.L. Wrana. 2001. TGF- $\beta$  induces assembly of a Smad2-Smurf2 ubiquitin ligase complex that targets SnoN for degradation. *Nat. Cell Biol.* 3:587–595.
- Di Guglielmo, G.M., C. Le Roy, A.F. Goodfellow, and J.L. Wrana. 2003. Distinct endocytic pathways regulate TGF- $\beta$  receptor signalling and turnover. *Nat. Cell Biol.* 5:410–421.
- Dong, C., Z. Li, R. Alvarez Jr., X.H. Feng, and P.J. Goldschmidt-Clermont. 2000. Microtubule binding to Smads may regulate TGF- $\beta$  activity. *Mol. Cell.* 5:27–34.
- Earnshaw, W., B. Bordwell, C. Marino, and N. Rothfield. 1986. Three human chromosomal autoantigens are recognized by sera from patients with anti-centromere antibodies. *J. Clin. Invest.* 77:426–430.
- Fang, G., H. Yu, and M.W. Kirschner. 1999. Control of mitotic transitions by the anaphase-promoting complex. *Philos. Trans. R. Soc. Lond. B Biol. Sci.* 354:1583–1590.
- Fry, A.M., and H. Yamano. 2006. APC/C-mediated degradation in early mitosis: how to avoid spindle assembly checkpoint inhibition. *Cell Cycle*. 5:1487–1491.
- Fukuchi, M., T. Imamura, T. Chiba, T. Ebisawa, M. Kawabata, K. Tanaka, and K. Miyazono. 2001. Ligand-dependent degradation of Smad3 by a ubiquitin ligase complex of ROC1 and associated proteins. *Mol. Biol. Cell*. 12:1431–1443.
- Gorbsky, G.J., R.H. Chen, and A.W. Murray. 1998. Microinjection of antibody to Mad2 protein into mammalian cells in mitosis induces premature anaphase. *J. Cell Biol.* 141:1193–1205.
- Gutierrez, G.J., and Z. Ronai. 2006. Ubiquitin and SUMO systems in the regulation of mitotic checkpoints. *Trends Biochem. Sci.* 31:324–332.
- Haglund, K., and I. Dikic. 2005. Ubiquitylation and cell signaling. *EMBO J.* 24:3353–3359.
- Han, G., A.G. Li, Y.Y. Liang, P. Owens, W. He, S. Lu, Y. Yoshimatsu, D. Wang, P. Ten Dijke, X. Lin, and X.J. Wang. 2006. Smad7-induced

beta-catenin degradation alters epidermal appendage development. *Dev. Cell.* 11:301–312.

Hernando, E., Z. Nahle, G. Juan, E. Diaz-Rodriguez, M. Alaminos, M. Hemann, L. Michel, V. Mittal, W. Gerald, R. Benezra, et al. 2004. Rb inactivation promotes genomic instability by uncoupling cell cycle progression from mitotic control. *Nature*. 430:797–802.

Howell, B.J., D.B. Hoffman, G. Fang, A.W. Murray, and E.D. Salmon. 2000. Visualization of Mad2 dynamics at kinetochores, along spindle fibers, and at spindle poles in living cells. *J. Cell Biol.* 150:1233–1250.

Howell, B.J., B. Moree, E.M. Farrar, S. Stewart, G. Fang, and E.D. Salmon. 2004. Spindle checkpoint protein dynamics at kinetochores in living cells. *Curr. Biol.* 14:953–964.

Jin, Y.H., E.J. Jeon, Q.L. Li, Y.H. Lee, J.K. Choi, W.J. Kim, K.Y. Lee, and S.C. Bae. 2004. Transforming growth factor-beta stimulates p300-dependent RUNX3 acetylation, which inhibits ubiquitination-mediated degradation. *J. Biol. Chem.* 279:29409–29417.

Kaneki, H., R. Guo, D. Chen, Z. Yao, E.M. Schwarz, Y.E. Zhang, B.F. Boyce, and L. Xing. 2006. Tumor necrosis factor promotes Runx2 degradation through up-regulation of Smurf1 and Smurf2 in osteoblasts. *J. Biol. Chem.* 281:4326–4333.

Kavsak, P., R.K. Rasmussen, C.G. Causing, S. Bonni, H. Zhu, G.H. Thomsen, and J.L. Wrana. 2000. Smad7 binds to Smurf2 to form an E3 ubiquitin ligase that targets the TGF beta receptor for degradation. *Mol. Cell.* 6:1365–1375.

Kee, Y., and J.M. Huibregtse. 2007. Regulation of catalytic activities of HECT ubiquitin ligases. *Biochem. Biophys. Res. Commun.* 354:329–333.

Malumbres, M., and M. Barbacid. 2007. Cell cycle kinases in cancer. *Curr. Opin. Genet. Dev.* 17:60–65.

Menssen, A., A. Epanchintsev, D. Lodygin, N. Rezaei, P. Jung, B. Verdoodt, J. Diebold, and H. Hermeking. 2007. c-MYC delays prometaphase by direct transactivation of MAD2 and BubR1: identification of mechanisms underlying c-MYC-induced DNA damage and chromosomal instability. *Cell Cycle*. 6:339–352.

Meraldi, P., V.M. Draviam, and P.K. Sorger. 2004. Timing and checkpoints in the regulation of mitotic progression. *Dev. Cell.* 7:45–60.

Michel, L.S., V. Liberal, A. Chatterjee, R. Kirchwegger, B. Pasche, W. Gerald, M. Dobles, P.K. Sorger, V.V. Murty, and R. Benezra. 2001. MAD2 haploinsufficiency causes premature anaphase and chromosome instability in mammalian cells. *Nature*. 409:355–359.

Michel, L., E. Diaz-Rodriguez, G. Narayan, E. Hernando, V.V. Murty, and R. Benezra. 2004. Complete loss of the tumor suppressor MAD2 causes premature cyclin B degradation and mitotic failure in human somatic cells. *Proc. Natl. Acad. Sci. USA.* 101:4459–4464.

Moren, A., T. Imamura, K. Miyazono, C.H. Heldin, and A. Moustakas. 2005. Degradation of the tumor suppressor Smad4 by WW and HECT domain ubiquitin ligases. *J. Biol. Chem.* 280:22115–22123.

Musacchio, A., and K.G. Hardwick. 2002. The spindle checkpoint: structural insights into dynamic signalling. *Nat. Rev. Mol. Cell Biol.* 3:731–741.

Nasmyth, K. 2005. How do so few control so many? *Cell*. 120:739–746.

Nefsky, B., and D. Beach. 1996. Pub1 acts as an E6-AP-like protein ubiquitin ligase in the degradation of cdc25. *EMBO J.* 15:1301–1312.

Nurse, P. 2000. A long twentieth century of the cell cycle and beyond. *Cell*. 100:71–78.

Ogunjimi, A.A., D.J. Briant, N. Pece-Barbara, C. Le Roy, G.M. Di Guglielmo, P. Kavsak, R.K. Rasmussen, B.T. Seet, F. Sicheri, and J.L. Wrana. 2005. Regulation of Smurf2 ubiquitin ligase activity by anchoring the E2 to the HECT domain. *Mol. Cell.* 19:297–308.

Peters, J.M. 2006. The anaphase promoting complex/cyclosome: a machine designed to destroy. *Nat. Rev. Mol. Cell Biol.* 7:644–656.

Ray, D., Y. Terao, D. Nimbalkar, L.H. Chu, M. Donzelli, T. Tsutsui, X. Zou, A.K. Ghosh, J. Varga, G.F. Draetta, and H. Kiyokawa. 2005. Transforming growth factor beta facilitates beta-TrCP-mediated degradation of Cdc25A in a Smad3-dependent manner. *Mol. Cell. Biol.* 25:3338–3347.

Rieder, C.L., A. Schultz, R. Cole, and G. Sluder. 1994. Anaphase onset in vertebrate somatic cells is controlled by a checkpoint that monitors sister kinetochore attachment to the spindle. *J. Cell Biol.* 127:1301–1310.

Schwamborn, J.C., M. Muller, A.H. Becker, and A.W. Puschel. 2007. Ubiquitination of the GTPase Rap1B by the ubiquitin ligase Smurf2 is required for the establishment of neuronal polarity. *EMBO J.* 26:1410–1422.

Shah, J.V., E. Botvinick, Z. Bonday, F. Furnari, M. Berns, and D.W. Cleveland. 2004. Dynamics of centromere and kinetochore proteins; implications for checkpoint signaling and silencing. *Curr. Biol.* 14:942–952.

Sotillo, R., E. Hernando, E. Diaz-Rodriguez, J. Teruya-Feldstein, C. Cordon-Cardo, S.W. Lowe, and R. Benezra. 2007. Mad2 overexpression promotes aneuploidy and tumorigenesis in mice. *Cancer Cell*. 11:9–23.

Stegmeier, F., M. Rape, V.M. Draviam, G. Nalepa, M.E. Sowa, X.L. Ang, E.R. McDonald III, M.Z. Li, G.J. Hannon, P.K. Sorger, et al. 2007. Anaphase initiation is regulated by antagonistic ubiquitination and deubiquitination activities. *Nature*. 446:876–881.

Stroschein, S.L., S. Bonni, J.L. Wrana, and K. Luo. 2001. Smad3 recruits the anaphase-promoting complex for ubiquitination and degradation of SnoN. *Genes Dev.* 15:2822–2836.

Subramaniam, V., H. Li, M. Wong, R. Kitching, L. Attisano, J. Wrana, J. Zubovits, A.M. Burger, and A. Seth. 2003. The RING-H2 protein RNF11 is overexpressed in breast cancer and is a target of Smurf2 E3 ligase. *Br. J. Cancer*. 89:1538–1544.

Taylor, S.S., and F. McKeon. 1997. Kinetochore localization of murine Bub1 is required for normal mitotic timing and checkpoint response to spindle damage. *Cell*. 89:727–735.

Tsutsui, T., B. Hesabi, D.S. Moons, P.P. Pandolfi, K.S. Hansel, A. Koff, and H. Kiyokawa. 1999. Targeted disruption of CDK4 delays cell cycle entry with enhanced p27kip1 activity. *Mol. Cell. Biol.* 19:7011–7019.

Vong, Q.P., K. Cao, H.Y. Li, P.A. Iglesias, and Y. Zheng. 2005. Chromosome alignment and segregation regulated by ubiquitination of survivin. *Science*. 310:1499–1504.

Wassmann, K., V. Liberal, and R. Benezra. 2003. Mad2 phosphorylation regulates its association with Mad1 and the APC/C. *EMBO J.* 22:797–806.

Yu, H. 2006. Structural activation of Mad2 in the mitotic spindle checkpoint: the two-state Mad2 model versus the Mad2 template model. *J. Cell Biol.* 173:153–157.

Zhu, H., P. Kavsak, S. Abdollah, J.L. Wrana, and G.H. Thomsen. 1999. A SMAD ubiquitin ligase targets the BMP pathway and affects embryonic pattern formation. *Nature*. 400:687–693.